

**Weierstraß-Institut**  
**für Angewandte Analysis und Stochastik**  
**Leibniz-Institut im Forschungsverbund Berlin e. V.**

Preprint

ISSN 2198-5855

**Bistability and hysteresis in an optically injected two-section  
semiconductor laser**

Alexander Pimenov<sup>1</sup>, Evgeniy A. Viktorov<sup>2</sup>, Stephen P. Hegarty<sup>3</sup>, Tatiana  
Habruseva<sup>4</sup>, Guillaume Huyet<sup>3</sup>, Dmitrii Rachinskii<sup>5</sup>, Andrei G. Vladimirov<sup>1</sup>

submitted: February 27, 2014

<sup>1</sup> Weierstrass Institute  
Mohrenstr. 39, 10117 Berlin, Germany  
E-Mail: alexander.pimenov@wias-berlin.de  
andrei.vladimirov@wias-berlin.de

<sup>2</sup> National Research University of ITMO  
St Petersburg, Russia

<sup>3</sup> Tyndall National Institute, University College Cork  
Lee Maltings, Dyke Parade, Cork, Ireland

<sup>4</sup> Aston University  
Aston Triangle, B4 7ET, Birmingham, UK

<sup>5</sup> Department of Mathematical Sciences, The University of Texas at Dallas  
800 W. Campbell Road, Richardson, Texas, USA

No. 1921  
Berlin 2014



---

2010 *Physics and Astronomy Classification Scheme*. 05.45.-a, 42.55.Px, 42.60.Fc, 42.65.Pc.

*Key words and phrases*. Bistability and hysteresis, numerical bifurcation analysis, semiconductor lasers, single-mode optical injection.

A. P. and A. G. V. acknowledge the support of SFB 787 of the DFG, project B5. T. H. acknowledges support of EU FP7 HARMOFIRE project, Grant No 299288. G. H., S. P. H. and A. G. V. acknowledge the support of EU FP7 PROPHET project, Grant No. 264687. A. G. V. and G. H. acknowledge the support of E. T. S. Walton Visitors Award of the SFI. G. H. and S. P. H. were also supported by the SFI under Contract No. 11/PI/1152, and under the framework of the INSPIRE Structured PhD Programme.

Edited by  
Weierstraß-Institut für Angewandte Analysis und Stochastik (WIAS)  
Leibniz-Institut im Forschungsverbund Berlin e. V.  
Mohrenstraße 39  
10117 Berlin  
Germany

Fax: +49 30 20372-303  
E-Mail: [preprint@wias-berlin.de](mailto:preprint@wias-berlin.de)  
World Wide Web: <http://www.wias-berlin.de/>

## Abstract

The effect of coherent single frequency injection on two-section semiconductor lasers is studied numerically using a model based on a set of delay differential equations. The existence of bistability between different CW and non-stationary regimes of operation is demonstrated in the case of sufficiently large linewidth enhancement factors.

## 1 Introduction

Multi-section semiconductor lasers have drawn sustained research interest for their utility in technological applications and as an experimental vehicle for the exploration of non-linear dynamics concepts. Material growth and device fabrication of semiconductor devices have matured rapidly, offering predictable and quantifiable material and device properties, even over wide operating parameter ranges. An important sub-category is that of two-section, mode-locked semiconductor lasers (MLLs), desired for their ability to generate better than picosecond optical pulses [1], with repetition rates reported from gigahertz to terahertz. Recently, a detailed experimental study has been carried out on two-section quantum-dot MLLs with optical injection. This study reported hysteresis between multiple regimes of operation such as stable mode-locking, modulated mode-locking, and single-mode lasing. This finding has implications for schemes aimed at improving laser coherence through optical injection, while also opening possibilities for exploiting these bistabilities as optical switches.

As a basic element for optical switches, bistable semiconductor lasers (SL) have been intensively studied for decades. Optically injected SL demonstrate multiple effects of bistability and hysteresis for both single mode [2, 3] and multimode devices [4]. Switches in optically injected multimode lasers have been investigated in [5]. Bistability and hysteresis in modelocked lasers have also been reported in active feedback lasers where the feedback is amplified in the external cavity [6].

In this paper we numerically investigate the dynamical states of multi-section devices under optical injection from a CW source. Using a travelling wave ring-cavity model that has been successfully applied to several semiconductor laser types, we identify the appearance of bistabilities and hysteresis between the locked states. We show that asymmetry in the phase-amplitude coupling in the gain and absorber sections is a fundamental requirement for the observation of hysteresis as experimentally reported for optically injected quantum dot (QD) lasers [7].

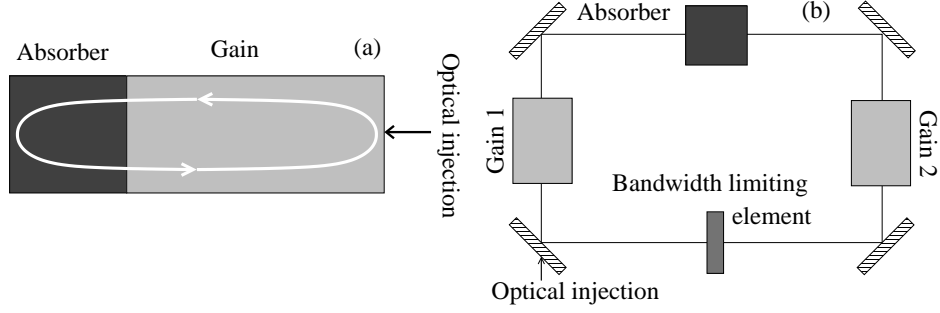


Figure 1: (a) Schematic representation of an optically injected two-section mode-locked laser. (b) Ring cavity model of an injected mode-locked laser.

## 2 Model equations

A schematic representation of a two-section laser subject to external injection from a single mode master laser is given in Fig. 1(a). The modeling of two-section lasers can be greatly simplified by treating the laser as a ring-cavity. Experimentally, optical injection of two-section mode-locked lasers [7] is typically from the gain section side, and thus amplified by this section before entering the absorber section. To account for this amplification, we consider the ring laser configuration shown in Fig. 1(b), where the gain section is split into two equal parts. The injected external signal first passes through a gain section, then through the absorber section and, finally, through the second gain section.

Extending the approach developed in [8–10] for two section mode-locked devices, we describe the laser configuration in Fig. 1(b) by a set of delay differential equations:

$$\gamma^{-1}\partial_t A(t) + A(t) = \sqrt{\kappa} \exp\left\{(1 - i\alpha_g)(G_1(t - T) + G_2(t - T))/2 - (1 - i\alpha_q)Q(t - T)/2\right\} \times A(t - T) + \eta \exp(2\pi i\nu t), \quad (1)$$

$$\tau_g \partial_t G_1(t) = g_0/2 - G_1(t) - (e^{G_1(t)} - 1) |A(t)|^2, \quad (2)$$

$$\tau_g \partial_t G_2(t) = g_0/2 - G_2(t) - e^{G_1(t) - Q(t)} \times (e^{G_2(t)} - 1) |A(t)|^2, \quad (3)$$

$$\tau_q \partial_t Q(t) = q_0 - Q(t) - s(1 - e^{-Q(t)}) e^{G_1(t)} |A(t)|^2, \quad (4)$$

where  $\partial_t$  denotes time derivative and the delay parameter  $T$  equals to the cold cavity round trip time. In Eqs. (1)-(4)  $A(t)$  is the normalized complex envelope of the electromagnetic field at the entrance of the first part of the gain section,  $G_1(t)$  and  $G_2(t)$  describe saturable gain introduced by the two gain sections,  $Q(t)$  is the saturable absorption introduced by the absorber section. The bandwidth of the spectral filtering is  $\gamma$  and the linewidth enhancement factor in the gain (absorber) section is  $\alpha_g$  ( $\alpha_q$ ).  $\tau_g = 500$  ps and  $\tau_q = 10$  ps are the relaxation times of the gain and absorber sections and are broadly representative of semiconductor lasers.  $s = 10$  is the typical ratio of the saturation intensities of the gain and absorption. The attenuation factor  $\kappa = 0.3$  describes the total non-resonant linear intensity losses per cavity round trip. The dimensionless parameters  $g_0 = 3.15$  and  $q_0 = 1.8$  describe linear unsaturated gain in the gain

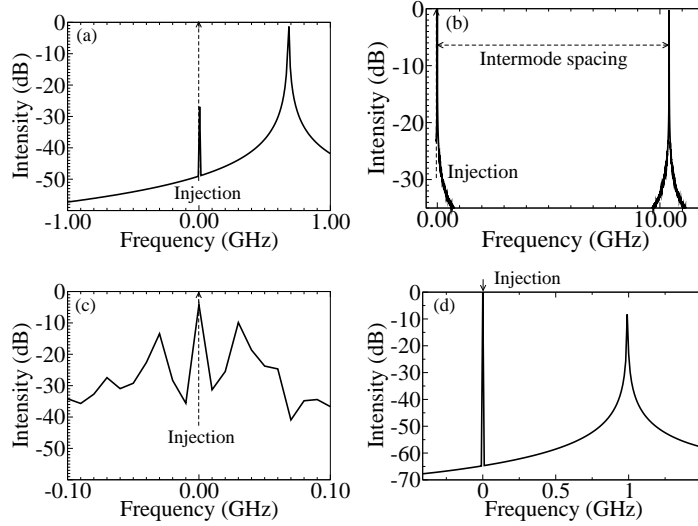


Figure 2: Optical spectra of injected two-section laser. Enlarged vicinity of the injection frequency in logarithmic scale.  $\eta = -40$  dB. (a) U: unlocked regime,  $\nu = -46.1549$  GHz. The beating between the laser modes and the injected field can be seen at a distance of  $1/10$  of the intermode spacing from the injection frequency. (b) ML: locked. The mode-locking tone is similar to U, but no beat tone exists,  $\nu = -45.4387$  GHz. (c) LM: locked modulated regime,  $\nu = -45.515$  GHz. (d) P: periodically modulated single mode,  $\nu = -45.4386$  GHz,  $\eta = -17.4598$  dB.

sections and linear unsaturated absorption in the absorber section, respectively. With these parameters, in the absence of external injection the laser operates in a mode-locking regime with the pulse repetition rate close to 10 GHz ( $T = 95.864$  ps).

The normalized injection rate  $\eta$  and the detuning  $\nu = \nu_{\text{inj}} - \nu_{\text{ref}}$  of the master laser signal  $\nu_{\text{inj}}$  from some reference frequency  $\nu_{\text{ref}}$  characterize the coherent optical injection. The reference frequency is set to zero at the maximum gain mode for  $\alpha_g = \alpha_q = 0$ .

### 3 Dynamical States

With the inclusion of optical injection in our simulations, a number of distinct dynamical states become apparent. The different regimes could be distinguished in the numerical simulations by computing the optical spectrum of the laser intensity. Representative optical spectra are displayed in Fig. 2. We identify five different regimes of operation.

**U: unlocked.** In this regime the impact of the injection upon the laser operation was inconsequential, with a weak beat tone developed between the injected light and the adjacent laser modes. The mode-locking frequency is the dominant feature of the power spectrum.

**ML: locked.** Here, the laser remains mode-locked, with one of the laser modes phase locked to the optical injection field. The beat tone between the injected field and the adjacent modes has disappeared and the mode-locking frequency is the only feature of the power spectrum.

**LM: locked-modulated.** In this regime, one laser mode is phase locked to the injection field, but

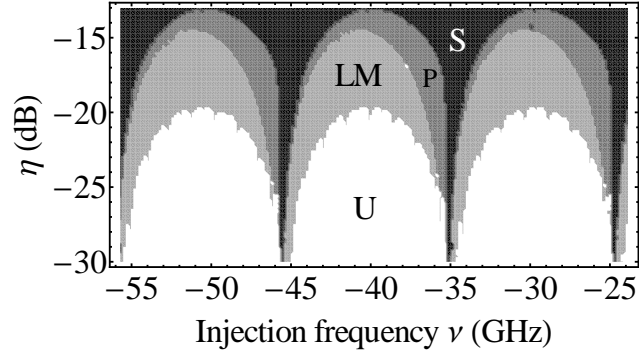


Figure 3: Different dynamical regimes calculated numerically for small values of the linewidth enhancement factors,  $\alpha_g = 2$  and  $\alpha_q = 0.7$ . In white areas “U” the laser is not locked to the external signal. White areas “U” corresponds to the mode-locking regimes very slightly affected by the external injection, while in light gray areas “LM” the laser is in locked modulated multi-mode regime. Dark gray areas “P” correspond to periodic single mode regimes with laser output intensity oscillating periodically at a frequency much smaller than the intermode frequency separation. CW regimes are indicated by black color (area “S”).

the mode-locking operation is no longer purely periodic, with the emergence of broad sidebands in the optical spectrum.

**P: periodic modulation.** In this regime the laser operates single-mode and the mode-locking is completely suppressed. The laser intensity is periodically modulated at a frequency substantially less than the mode-locking frequency.

**S: single mode.** In this regime the laser operates with a single, unmodulated mode.

The great variety of operating regions in our system suggests using multiple control parameters, that can be collected into three groups. The frequency interval in which locking takes place will be referred to as the locking range, the normalized injection rate  $\eta$  controls the size of the locking range, as in the other optical injection problems. The linewidth enhancement factors  $\alpha_g$  and  $\alpha_q$  affect the symmetry of the locking boundaries and control the appearance of hysteresis. Finally, we use the spectral filtering bandwidth  $\gamma$  as a suitable control parameter to characterize the hysteresis area, and to confirm the relevance of the scaling law for hysteresis in our multidimensional system.

Fig. 3 shows how these regimes are organized in the  $\nu$ - $\eta$  plane. The major domains are mapped and labelled using the key given above. These domains were obtained by numerical integration of Eqs. (1)-(4) with rather small linewidth enhancement factors,  $\alpha_g = 2$  and  $\alpha_q = 0.7$ , using the following procedure: for a given injection rate, the injection detuning  $\nu$  was first increased stepwise from  $\nu = -55$  GHz to  $\nu = -25$  GHz and then decreased from  $\nu = -25$  GHz back to  $\nu = -55$  GHz. For each value of  $\nu$  the solution calculated at the previous  $\nu$ -value was taken as an initial condition. It is seen from Fig. 3 that each laser mode gives rise to a separate “locking tongue”, i.e. a narrow wedge-shaped area where the frequency of this mode can be locked to the frequency of the external injection  $\nu$  (black and dark gray areas). The results presented in Fig. 3 are in a qualitative agreement with the results of experimental measurements at low

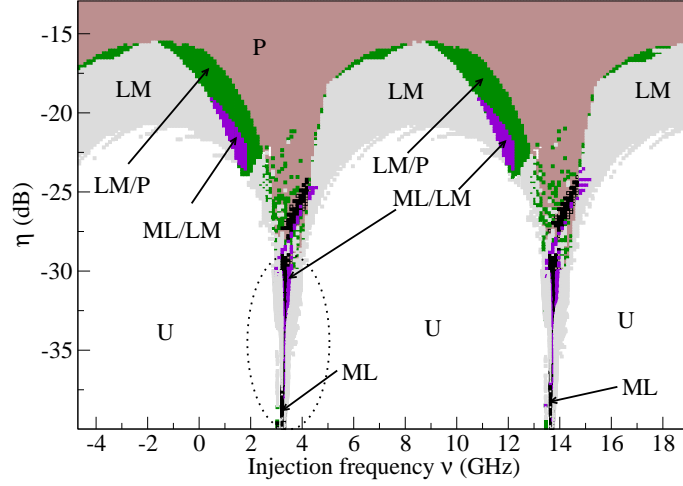


Figure 4: Domains of different operation regimes calculated numerically for  $\alpha_g = 13$  and  $\alpha_q = 3.5$ . Area “P” corresponds to time-periodic single mode regimes locked to the injection frequency, black areas “ML” – to mode-locked regimes synchronized to the injection frequency, areas “LM” – to multimode regimes with modulated laser intensity. Other colored areas show bistability domains between different operation regimes: “LM/P” – modulated/periodic, “ML/LM” – mode locked/modulated.

injection powers [7], and show no bistability between the different regimes of operation.

The map presented in Figs. 4 and 5 are similar to that shown in Fig. 3, but correspond to larger values of the linewidth enhancement factors in the gain and absorber sections,  $\alpha_g = 13$  and  $\alpha_q = 3.5$ . It is seen that at large injection rate, instead of CW regimes indicated by the letter “S” in Fig. 3, we have periodically modulated single-mode regimes, see area “P” in Fig. 4. For the values of linewidth enhancement factors corresponding to Fig. 4, CW regimes appear at much higher injection rates ( $\eta > -13$  dB) than for the parameter values of Fig. 3, therefore, these regimes are not shown in Fig. 4. Fig. 5 presents an enlarged view of the area encircled by the dashed line in Fig. 4. In these two figures in the domain indicated by “ML/LM” the laser exhibits a bistability between locked modulated multimode and mode-locked regimes. Furthermore, in the areas labeled “LM/P” in Fig. 4 single mode periodically modulated regimes are bistable with locked modulated multimode ones. The corresponding branches of solutions are presented Fig. 6. The cusp catastrophe induced bistability is normally expected in a system with strong asymmetry. Such an asymmetry in the two-section device can be attributed to sufficiently different strength of the phase-amplitude coupling in the gain and absorber section. We find that significant difference between  $\alpha_g$  and  $\alpha_q$  is a necessary condition for bistable operations in our system.

## 4 Hysteresis

We have analyzed the bifurcations leading to bistability of CW and periodically modulated single mode regimes at high injection rates beyond the range shown in Fig.3. In order to perform the

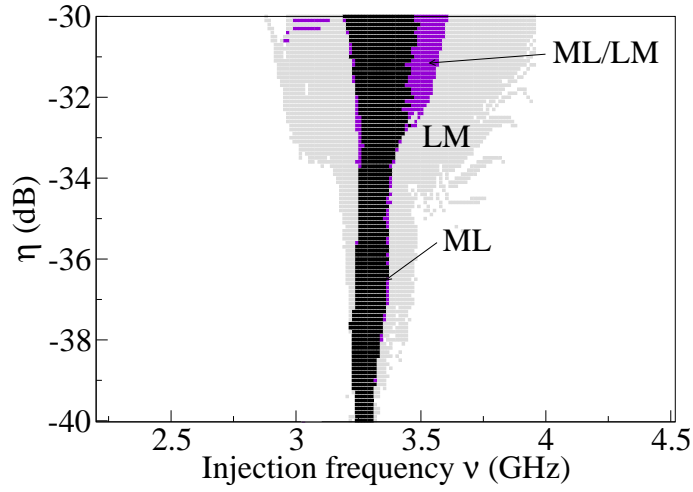


Figure 5: Zoom of one of the locking tongues shown in Fig. 4 at small injection rate. Bistability domains between locked modulated and mode-locked solutions are indicated “ML/LM”. Black area “ML” corresponds to the domain of mode-locking regimes locked to the injection frequency.

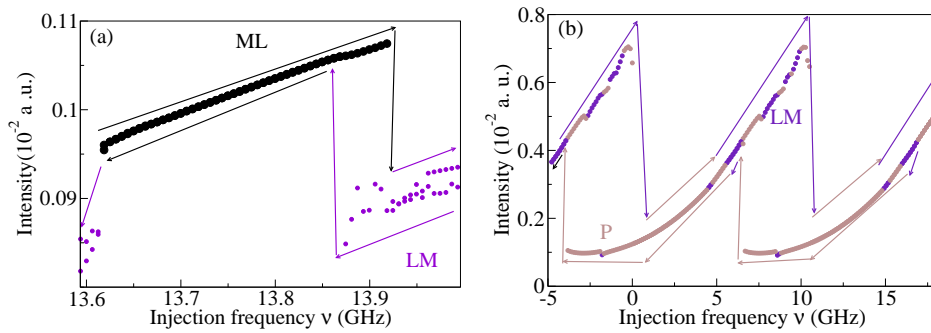


Figure 6: Bistability between different laser operation regimes. Arrows indicate the direction, in which the frequency detuning  $\nu$  is changed. a)  $\eta = -32.2185$  dB. Small circles represent locked modulated multimode regime, big circles represent the mode-locked regime. When the detuning is increased the transition from mode-locked regime (big circles) to locked modulated regime (small circles) occurs at  $\nu \approx 13.92$  GHz, whereas when the detuning is decreased the opposite transition from locked modulated regime to mode-locked regime takes place at  $\nu \approx 13.87$  GHz. b)  $\eta = -13.9794$  dB. Dark points – locked modulated regimes, light – periodic regimes. When the detuning is decreased, a transition from periodic regime to locked modulated regime occurs at  $\nu \approx 6$  GHz, whereas when the detuning is increased the opposite transition takes place at  $\nu \approx 10$  GHz.



analysis, we have used the path-following software package DDE-BIFTOOL [11]. The branch of single-mode solutions obtained by changing the injection detuning parameter  $\nu$  is shown in Fig. 7(a). It is seen that when the detuning  $\nu$  is changed the laser intensity oscillates almost periodically on this branch with the period around the free spectral range  $1/T$ . Each oscillation period of the branch contains two segments corresponding to a stable CW solution: one of them bounded by a fold bifurcation point A from the right side and by an Andronov-Hopf bifurcation point D from the left side, and the other is bounded by an Andronov-Hopf bifurcation point C from the right side and by a fold point B from the left side. These segments are indicated by solid black lines. Between points D and C the branch of CW solutions is unstable with respect to a self-pulsing instability (dashed line). It is seen from Fig. 7(a) that there is a bistability between CW and periodically modulated single mode solutions within certain frequency ranges. The origin of this bistability can be understood by noticing that a part of the CW branch BCDAB demonstrates a typical example of nonlinear resonance behavior with resonant frequency close to the frequency of the corresponding longitudinal laser mode. Due to the multiplicity of the modes the CW branch exhibits multiple resonances each corresponding to a certain longitudinal mode of a mode-locked laser. In the case of nonzero linewidth enhancement factors, modal frequencies depend on the injection amplitude. In particular, it is seen from Fig. 7(a), that in the case when  $\alpha_g > \alpha_q > 0$  modal frequencies increase with the injection rate  $\eta$ . This dependence of modal frequencies on the injection rate can lead to an overlap of the resonances corresponding to neighboring longitudinal modes and, hence, to the appearance of bistability and hysteresis. Therefore, experimental observations of bistability and hysteresis in an optically injected QD mode-locked laser [7] are consistent with the earlier experiments indicating that the  $\alpha$ -factor in the QD based semiconductor gain noticeably increases above threshold [12, 13] and also with the theoretical analysis of the present paper. As one can see in Fig. 7(b), the overlap of the resonances corresponding to neighboring longitudinal modes appears between two fold bifurcation points, A and B, when the absolute value of the difference of the two linewidth enhancement factors  $|\alpha_g - \alpha_q|$  is sufficiently large. With the decrease of the linewidth enhancement factor  $\alpha_g$  in the gain section the two fold bifurcations corresponding to lines A and B come closer and closer to one another and, finally, merge and annihilate at the cusp bifurcation point P. Below this point there is no bistability and hysteresis in the model. The presence of bistability at sufficiently large linewidth enhancement factors assumes abrupt jumps between the solutions corresponding to neighboring longitudinal modes. Similar jumps between CW and periodically modulated single mode regimes were observed experimentally and demonstrated theoretically in a multimode semiconductor laser without a saturable absorber section [5].

The cusp hysteresis has been observed in numerous dynamical systems, and possesses some universal scaling laws for hysteresis loop area (width). In order to characterize the cusp hysteresis in Fig. 7, we chose the filter bandwidth  $\gamma$  as a control parameter. The bifurcation diagram in Fig. 7 remains largely unchanged for a broad range of the  $\gamma$  change, which allows appropriate calculation of the hysteresis width as a function of the control parameter. The results are shown in Fig. 8 for different values of the detuning  $\nu$ . The hysteresis width  $H(\gamma)$  is given by  $H(\gamma) = H_0 + C\gamma^{-\beta}$ . The scaling exponent  $\beta$  remains the same for a small variation of  $\nu$  around the optical spectrum peak ( $\nu = 0$  GHz and 15 GHz), but increases for the injections closer to the side modes away from the peak ( $\nu = 95$  GHz). It indicates that the weaker side modes are more sensitive to the injection with a faster change of the hysteresis area.

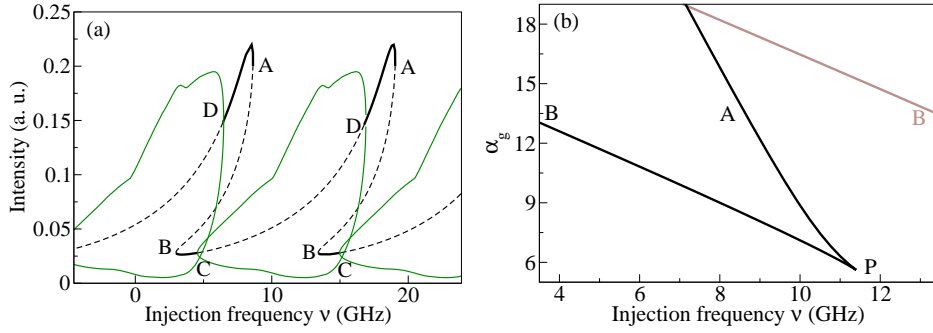


Figure 7: Bifurcation diagrams for Eqs. (1)-(4) obtained numerically using the software package DDE-BIFTOOL. The injection is strong,  $\eta = -6.0206$  dB. Other parameters are the same as on Fig. 4. a) Branches of CW and periodically modulated single mode solutions. Stable and unstable parts of the CW branch are shown by black solid thick and dashed lines, respectively. Solid thin lines represent minima and maxima of solutions with time-periodic intensity. A and B indicate fold bifurcations, C and D – Andronov-Hopf bifurcations. b) Bistability domain is located between two fold bifurcation lines, A and B. P is the codimension-two cusp bifurcation point.

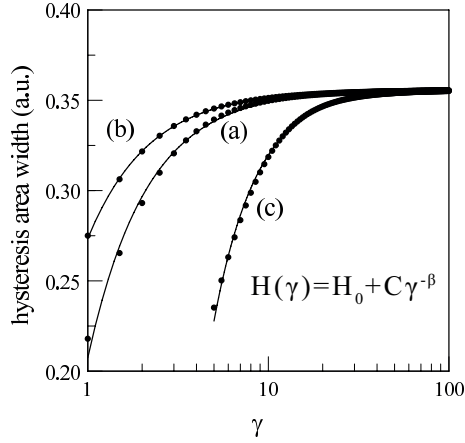


Figure 8: Numerical results (dots) and corresponding fits (solid lines) for the width of the hysteresis area in Fig. 7 as a function of the bandwidth  $\gamma$ . The scaling exponent  $\beta$  is 1.3 for  $\nu = 0$  (a) and 15GHz (b), and 1.8 for  $\nu = 95$ GHz (c).

## 5 Conclusion

To conclude, using a modification of delay differential mode-locking model proposed in [8–10] we have performed a numerical study of the operation regimes of an optically injected semiconductor mode-locked laser. We have shown that similarly to reported experimental results [7], [14] bistability and hysteresis can exist between different laser operation regimes. This bistability appears at sufficiently large values of the linewidth enhancement factor in the gain section and is related to overlapping nonlinear resonances corresponding to different longitudinal laser modes. When the linewidth enhancement factor in the gain section is sufficiently small, there is no bistability in the model equations.

## References

- [1] E. U. Rafailov, M. A. Cataluna, and W. Sibbett, *Nature Photonics* **1**, 395-401 (2007).
- [2] T. Erneux, E. A. Viktorov, B. Kelleher, D. Goulding, S. P. Hegarty, and G. Huyet, *Optics Letters*, "Optically injected quantum dot lasers", **35**, 937 (2010).
- [3] A. Hohl, H. J. C. van der Linden, R. Roy, G. Goldsztein, F. Broner, and S. H. Strogatz, "Scaling Laws for Dynamical Hysteresis in a Multidimensional Laser System," *Phys. Rev. Lett.* **74**, 2220–2223 (1995)
- [4] P. Heinrich, B. Wetzel, S. O'Brien, A. Amann, S. Osborne, "Bistability in an injection locked two color laser with dual injection," *Appl. Phys. Lett.* **99**, 011104 (2011).
- [5] J. K. White, J. V. Moloney, A. Gavrielides, V. Kovanis, A. Hohl, and R. Kalmus, "Multilongitudinal-Mode Dynamics in a Semiconductor Laser Subject to Optical Injection," *IEEE J. Quantum Electron.* **34**, 1469-1473 (1998).
- [6] S. Bauer, O. Brox, J. Kreissl, B. Sartorius, M. Radziunas, J. Sieber, H.-J. Wünsche, and F. Henneberger. Nonlinear dynamics of semiconductor lasers with active optical feedback. *Phys. Rev. E*, **69**, 016206 (2004).
- [7] T. Habruseva, S. P. Hegarty, A. G. Vladimirov, A. Pimenov, D. Rachinskii, N. Rebrova, E. A. Viktorov, G. Huyet, "Bistable regimes in an optically injected mode-locked laser", *Opt. Express* **20**, 25572-25583 (2012).
- [8] A. G. Vladimirov and D. Turaev, "Model for passive mode locking in semiconductor lasers," *Phys. Rev. A* **72**, 033808 (2005)
- [9] A.G. Vladimirov, D. Turaev, and G. Kozyreff, "Delay differential equations for mode-locked semiconductor lasers," *Optics Letters* **29**, 1221-1223 (2004)
- [10] A.G. Vladimirov and D. Turaev, "A new model for a mode-locked semiconductor laser," *Radiophysics and Quantum Electronics*, **47**, 10-11, 769-776 (2004)

- [11] K. Engelborghs, T. Luzyanina, and D. Roose, "Numerical bifurcation analysis of delay differential equations using DDE-BIFTOOL," *ACM Trans. on Mathematical Software* 28, 1, 1-21 (2002).
- [12] T. Piwonski et al., "Ultrafast gain and refractive index dynamics in GaInNAsSb semiconductor optical amplifiers," *J. Appl. Phys.* 106, 083104 (2009).
- [13] Dagens, B. A. Markus, J.X. Chen, J.-G. Provost, D. Make, O. Le Gouezigou, J. Landreau, A. Fiore, B. Thedrez, *Electr.Lett.*, 41, 323(2005).
- [14] A. Hurtado, M. Nami, I. D. Henning, M. J. Adams, L. F. Lester, "Bistability patterns and nonlinear switching with very high contrast ratio in a 1550nm quantum dash semiconductor laser", *Appl. Phys. Lett.* **101**, 161117 (2012).